

July 19, 2006

Experimental and numerical investigation of nanoparticle removal using acoustic streaming and the effect of time

Kaveh Bakhtari

Northeastern University - NSF Center for Microcontamination Control

Rasim O. Guldiken

Northeastern University - NSF Center for Microcontamination Control

Prashanth Makaram

Northeastern University - NSF Center for Microcontamination Control

Ahmed A. Busnaina

Northeastern University - NSF Center for Microcontamination Control

Jin-Goo Park

Hanyang University, South Korea - Dept. of Materials and Chemical Engineering

Recommended Citation

Bakhtari, Kaveh; Guldiken, Rasim O.; Makaram, Prashanth; Busnaina, Ahmed A.; and Park, Jin-Goo, "Experimental and numerical investigation of nanoparticle removal using acoustic streaming and the effect of time" (2006). *Center for High-Rate Nanomanufacturing Publications*. Paper 13. <http://hdl.handle.net/2047/d20000924>



Experimental and Numerical Investigation of Nanoparticle Removal Using Acoustic Streaming and the Effect of Time

Kaveh Bakhtari,^a Rasim O. Guldiken,^a Prashanth Makaram,^a
Ahmed A. Busnaina,^{a,*} and Jin-Goo Park^{b,*}

^aNSF Center for Microcontamination Control, Northeastern University, Boston, Massachusetts 02115

^bDepartment of Materials and Chemical Engineering, Hanyang University, Ansan 426-791, South Korea

The removal of nanoparticles is becoming increasingly challenging as the minimum linewidth continues to decrease in semiconductor manufacturing. In this paper, the removal of nanoparticles from flat substrates using acoustic streaming is investigated. Bare silicon wafers and masks with a 4 nm silicon cap layer are cleaned. The silicon-cap films are used in extreme ultraviolet masks to protect Mo-Si reflective multilayers. The removal of 63 nm polystyrene latex (PSL) particles from these substrates is conducted using single-wafer megasonic cleaning. The results show higher than 99% removal of PSL nanoparticles. The results also show that dilute SC1 provides faster removal of particles, which is also verified by the analytical analysis. Particle removal from the 4 nm Si-cap substrate is slightly more difficult as compared to bare silicon wafers. The experimental results show that the removal of nanoparticles takes a relatively long removal time. Numerical simulations showed that the long time is due to particle oscillatory motion and redeposition, and that this phenomenon is not observed in the removal of sub- μm or larger size particles. © 2006 The Electrochemical Society. [DOI: 10.1149/1.2217287] All rights reserved.

Manuscript submitted January 9, 2006; revised manuscript received April 24, 2006. Available electronically July 19, 2006.

Fabrication of micro- and nanoelectronics requires nanoscale particle and other contaminant removal from wafers and associated thin films. These undesired particles on the wafer surface influence the device yield and reliability. These particles could result from chemical vapor deposition, physical vapor deposition, etching processes, and many other fabrication processes. The FEOL (front end of the line) critical particle size is expected to decrease to 9 nm by the year 2018.¹ The smaller the particles, the harder it is to overcome the adhesion force between the particle and the substrate. The adhesion force consists of the van der Waals and the electrostatic double-layer forces. High-frequency sonic energy in liquids (megasonic cleaning) has proven to be an effective method for particle removal. Although megasonic cleaning is widely used in the semiconductor industry, the fundamental physical processes are not thoroughly understood. Olaf² made early observations of sonic cleaning of glass surfaces in the range from 15 kHz to 2.5 MHz. McQueen³ recognized the importance of acoustic streaming and the thin boundary layer thickness in small particles removal from surfaces. Busnaina and Kaskoush⁴ found that increasing the frequency above 300 kHz could eliminate the surface damages on wafer surfaces during wafer cleanings. Gale and Busnaina⁵ studied the mechanisms of particle removal in megasonic and ultrasonic cleaning, including the effects of frequency, temperature, and power density.

Acoustic streaming is considered to be the key cleaning mechanism in the removal of sub- μm particles.⁶⁻⁸ According to Olim,⁹ theoretically it is not possible to remove particles below 100 nm using megasonic cleaning. But, in practice, particle sizes down to and less than 100 nm have been effectively removed using megasonics. The underestimation of Olim's model is because the viscous drag force and the double-layer force are not included in the model. Preliminary experiments for the removal of nanoscale particles (90, 63, and 28 nm PSL, polystyrene latex particles) are conducted using single-wafer megasonic cleaning by Busnaina and Bernard.¹⁰ Lin¹¹ has developed theoretical models to predict removal rates of nanoparticles from silicon wafers.

In this paper, extreme ultraviolet (EUV) masks and bare silicon wafers are used in the experiments. Cleaning of EUV masks is more challenging because the surface cleanliness requirements for EUV masks are much more stringent than silicon wafers (zero particles at 30 nm). In this study, we seek a better understanding of the particle-fluid interaction and the nanoscale particle removal mechanism. One

important issue is the removal time, which is observed to be unusually long for nanoscale particles. Cleaning time has not been an issue when dealing with micro or sub- μm particles using acoustic streaming. Force and moment analysis on the particle provides a theoretical model for particle detachment. The particle removal model (moment ratio model) used in this paper could predict when an applied force is sufficient for particle removal based on the moment ratio. Both experiments and computational fluid dynamics (CFD) simulations have been used to develop a better understanding of nanoparticle removal from flat substrates using pulsating flow.

Particle removal in high-frequency sonic cleaning relies on acoustic streaming and the reduction of the boundary layer thickness above the substrate. The thickness of the acoustic boundary layer is very small compared to a typical hydrodynamic boundary layer at the same velocity.

Figure 1 compares the velocity profile for laminar, turbulent, and acoustic flows at a distance of 4 in. (10 cm) from the leading edge of the plate using a velocity of 4 m/s at a frequency of 800 kHz.¹¹

The acoustic boundary layer thickness, δ_{ac} , is a function of the viscosity of the media ν and the frequency of oscillation f

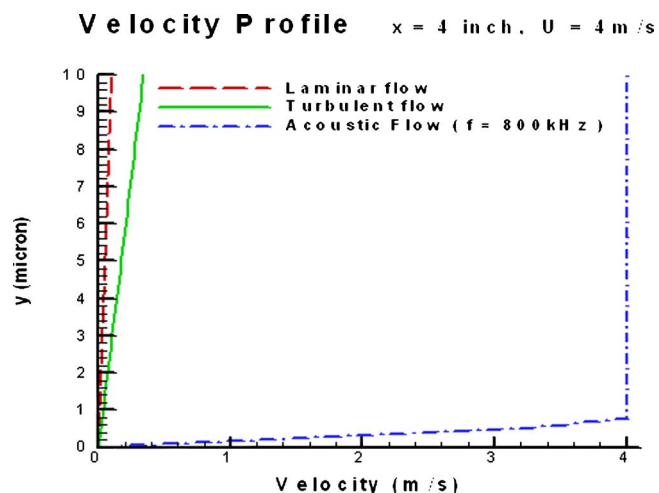


Figure 1. Comparison of hydrodynamic and acoustic boundary layers (Ref. 11).

* Electrochemical Society Active Member.

^z E-mail: busnaina@neu.edu

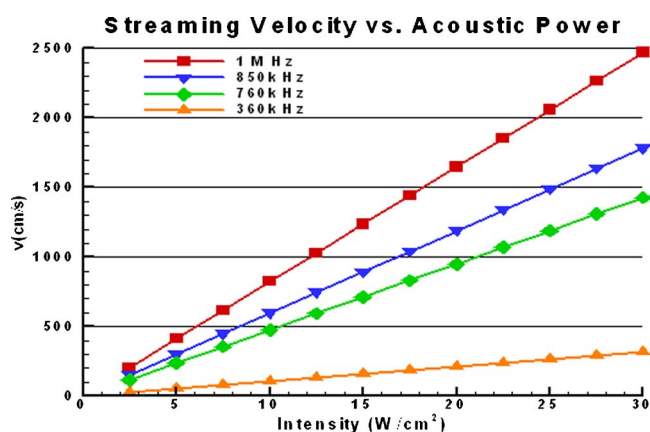


Figure 2. Streaming velocity as a function of acoustic power and frequency.

$$\delta_{ac} = \sqrt{\frac{2\nu}{\omega}} \text{ where } \omega = 2\pi f \quad [1]$$

Hydrodynamic boundary layer thickness, δ , for turbulent flow is given by

$$\delta = 0.16 \left(\frac{\nu}{Ux} \right)^{1/7} x \quad [2]$$

where U is the fluid velocity and x is the distance from the leading edge of the wafer.

The thin boundary layer allows the particles to be exposed to a much higher velocity as compared to particles in a hydrodynamic boundary layer. The equations also show that unlike the hydrodynamic case the acoustic boundary layer thickness is not a function of distance and is uniform along the wafer. The other important factor in the particle removal mechanism is the streaming velocity. Acoustic pressure waves can be considered as attenuated plane waves traveling between two parallel planes. The single-wafer megasonic tank will behave as a closed-ended channel.

Sound at high intensity levels in gases and liquids are accompanied by second-order steady flow patterns known as acoustic streaming. It is due mainly to viscous attenuation but also related to wave interaction with solid boundaries.

Acoustic streaming velocity, u , at the center of the tank is defined as¹²

$$u = B \left(\frac{h^2}{4} - z_1^2 \right) - K \frac{h^2}{8\mu} \quad [3]$$

$$K = \mu B (2 - 3Z_1^2 + Z_1^3) \quad Z_1 = 2z_1/h \quad B = \frac{8\Pi^2 I f^2}{3\rho c^4}$$

where ρ is the density of the media, c is the speed of sound in the liquid, μ is the viscosity of the media, I is the intensity of megasonic wave, f is the frequency of the megasonic wave, z_1 the distance between the wall and the center of the tank, and h the distance between the walls of the tank. As Eq. 1 and 3 show, higher frequency increases the acoustic streaming velocity while decreasing the boundary layer thickness, thus exposing nanoscale particles to higher streaming velocities. Figure 2 shows the increase in streaming velocity as a function of the acoustic power intensity for fixed megasonic frequencies.

There are three different mechanisms for particle removal: sliding, rolling, or lifting. The megasonic cleaning creates a tangential drag force on the particle which results in particle removal by the rolling mechanism.

Figure 3 presents the force and moments applied on a single particle from the acoustic streaming flow. In this figure Δ is the

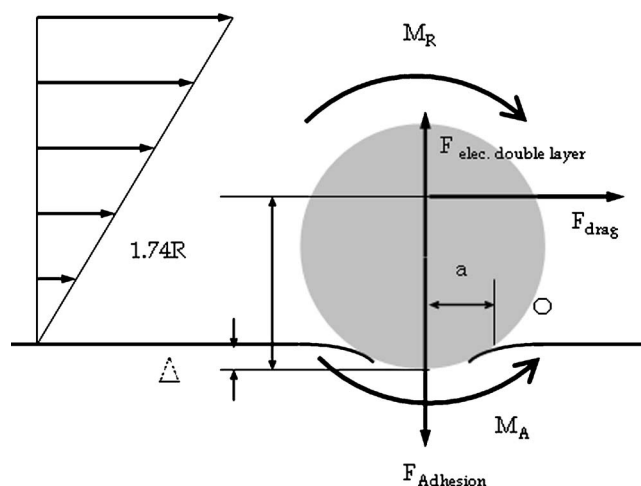


Figure 3. MR model for the removal of particles from the surface.

deformation height of the particle. The ratio of the removal moment to the adhesion resisting moment, MR, is given by

$$MR = \frac{F_d(1.74R - \Delta) + F_{dl} \cdot a}{F_a \cdot a} \quad [4]$$

where MR is the moment ratio, Δ is the deformation height of the particle, a is the contact radius between the deformed particle and the surface, F_d is the drag force, F_{dl} is the double-layer force, and F_a is the adhesion force.

When the removal moment overcomes the adhesion moment, theoretically, the particle is removed by rolling. The drag moment acting on the particle will lead the particle to roll over and detach from the surface.¹³

Present understanding of particle adhesion is dominated by three theories: DMT (Derjaguin-Muller-Toporov), JKR (Johnson-Kendall-Roberts), and MP (Maugis and Pollock) models. The JKR and DMT models are used to describe adhesion of elastically deforming system. The MP model accounted for tensile interactions and plastic deformations.

The adhesion of submicron or nanoparticles is dominated by the van der Waals force, which is given by¹⁴

$$F_{vdw} = \frac{AR}{6z_0^2} \quad [5]$$

The attractive force F_{vdw} deforms the interface and a circular adhesion area is formed between the adherents. The equation above does not take into account the adhesion force component due to deformation. Bowling¹⁵ gave the total adhesion force including the component due to the deformation as

$$F_{ad} = F_{vdw} + F_{vdw-deform} = \frac{AR}{6z_0^2} \left(1 + \frac{a^2}{Rz_0} \right) \quad [6]$$

where A is the Hamaker constant, R is the radius of the spherical particle, z_0 is the separation distance between the particle and the substrate (for smooth surfaces, it is taken as 4 Å) and a is the contact radius between the deformed particle and the surface.

Both JKR and DMT have their ranges of validity. The range of each theory is defined in terms of a dimensionless parameter μ .^{16,17} The actual value of the contact radius predicted by the JKR theory is approximately twice that predicted by the DMT model. So, it is necessary to establish which theory correctly describes a system. Maugis and Pollock expanded the JKR model to the plastic region. Since PSL is a relatively soft material, the adhesion-induced deformation could be significant. Large deformation leads to a higher adhesion force and a more difficult removal process. The MP model

is the most suited particle substrate system for calculating the adhesion force for PSL/Si particle and substrate system.¹⁸

The last concept in understanding the adhesion and removal mechanism is the double-layer force. Particles and surfaces immersed in a liquid are charged by the adsorption of the ions in the solution. An equal but oppositely charged layer in the adjacent liquid balances this charge on the surface of the immersed substrate, resulting in a so-called electrical double layer. The Hogg-Healy-Fuerstenau (HHF) approximation,¹⁹ which is based on the one-dimensional linear Poisson-Boltzmann and Debye-Hückel equation, is commonly used. At small separation distances between the particle and substrate the HHF model overestimates the double-layer force. The following equation, compression approximation,^{20,21} is the appropriate double-layer force expression for the nanoparticle-substrate model because it shows the force between flat plates under the constant charge assumption

$$F(D) = \frac{4\pi R\rho_z KT}{\kappa} \left\{ 2Y \ln \left(\frac{B + Y \coth(\kappa D/2)}{1 + Y} \right) - \ln[Y^2 + \cosh(\kappa D) + B \sinh(\kappa D)] + \kappa D \right\} \quad \text{where } Y = (y_1 + y_2)/2 \text{ and } y = z_e\psi/kT \text{ and } B = [1 + Y^2 \csc^2 h^2(\kappa D/2)]^{1/2} \quad [7]$$

and κ is the reciprocal of the Debye length, which is given by

$$\kappa^2 = \sum_i \frac{\rho_{z_i} e^2 z_i^2}{\epsilon \epsilon_0 K T}$$

Direct measurement results have shown that constant surface charge boundary condition describes the electrical double-layer interaction much better than the constant surface potential boundary condition at small separation between the two surfaces.

Experimental

Red fluorescent 63 nm PSL particles are deposited on 200 mm bare silicon wafers using a nebulizer. The wafer is then cleaned using acoustic streaming utilizing a single-wafer megasonic tank with a frequency of 760 kHz. An optical automated scanning microscope, Nikon Optiphot 200D, modified for fluorescent visualization attachment with a cooled camera to scan fluorescent particles, is used to count the particles. Image Pro-plus software is used to count the particles located at a specified location on the wafer before and after cleaning. To verify the nanoparticle counting technique by the fluorescent microscopy, field emission scanning electron microscope (FESEM) images of nanoparticles are compared to the fluorescent image at the same location. Fluorescent microscopy images at 1000 times magnification of a 63 nm fluorescent PSL particles on a wafer are verified using FESEM at 45,000 times at the same location on the wafer.²²⁻²⁴

Either deionized (DI) water or SC1 is used and circulated in the single-wafer megasonic tank using a closed-loop system passing through a pump and a 100 nm filter.

Two different flat substrates are used; the first one is an 8 in. bare silicon wafer and the second is an 8 in. wafer with a 4 nm Si-cap film. This automated stage can scan the same exact locations before and after cleaning. Five locations on the wafer with dimensions of 2000 by 2000 μm are specified and the particles are counted at each location before and after cleaning. The removal efficiency is then averaged over all five locations to get the average removal efficiency for the wafer. An example of the average number of 63 nm particles before and after cleaning for a bare silicon wafer, using single-wafer megasonics for 3 min in DI water at 25°C is as follows:

Number of particles before cleaning: 7881 (averaged over five locations)

Number of particles after cleaning: 296 (averaged over five locations)

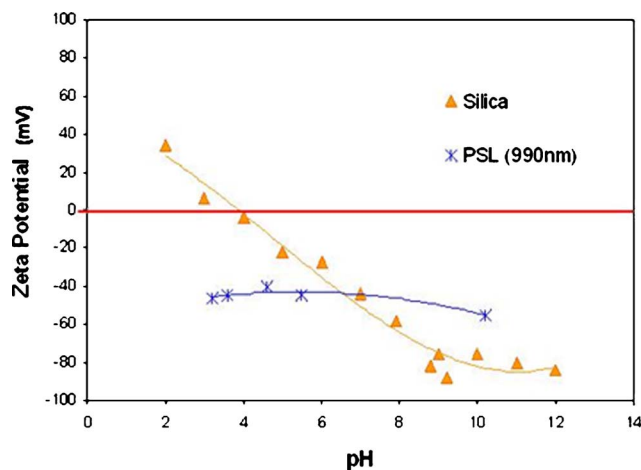


Figure 4. Zeta potential measurements as a function of pH of the solution.

Simulation of Particle Removal and Transport

Computational and analytical models are used to calculate the bulk acoustic streaming velocity in the megasonic tank. Instead of modeling the streaming velocity as a half-sinusoidal oscillating flow velocity, the piezoelectric transducers located at the bottom of the tank are modeled as a moving boundary condition. This way, the pressure waves and the acoustic streaming are all captured in the simulation, resulting in a more accurate model for acoustic streaming in a megasonic tank than other models developed or used by others. The grid deformation module with automatic remesh is used to model the moving boundary. This method uses a standard transfinite interpolation scheme to determine the interior node distribution based on the motion of the boundary nodes.

Another unique feature used in this simulation is the free-surface boundary condition at the liquid-gas interface instead of a far-field boundary condition. This boundary condition allows the traveling pressure waves to produce surface waves on the water surface. Therefore, in this model, all the acoustic streaming velocity and thin acoustic boundary layers are induced by the transducer vibration and not imposed on the flow field.

The induced streaming velocity in the tank is then used to calculate the drag force and the removal moment applied on the particle. The double-layer force is also calculated based on the zeta potential and the pH of the cleaning solution. Figure 4 shows the measured zeta potential of PSL and silica as a function of the pH of the solution. SC1 and DI water are used in the experiments. SC1 has a higher pH value than DI water. According to Fig. 4, the higher pH results in a larger negative charge for zeta potential for both the silica substrate and the PSL particle. This larger absolute value for zeta potential results in a larger repulsive double-layer force and eventually a larger moment ratio. The rolling moment removal mechanism has been shown as the mechanism that requires the least force for particle removal.^{25,26} After calculating the drag force, the adhesion, and double-layer force, the MR is determined.

The simulation is also used to track the particles after detachment and predict particle trajectory, particle redeposition, readhesion, and subsequent detachment. The MR is used to indicate when particle adhesion and detachments occurs. The particle tracking continues until the particle leaves the tank.

Results and Discussion

The removal of 63 nm PSL particles on bare silicon and 4 nm Si-capping layer wafers have been investigated. The MR values for DI water and dilute SC1 chemistry (1:2:40 ammonium hydroxide, hydrogen peroxide and DI water) are as follows:

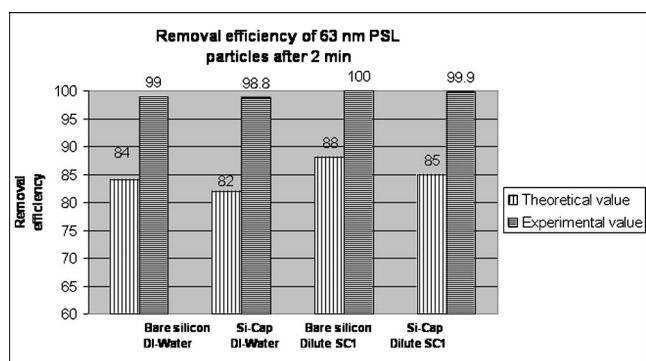


Figure 5. Experimental and theoretical particles removal efficiency values.

Bare silicon: MR = 1.2 for DI water and MR = 1.37 for SC1 solution.

4 nm Si-Capping layer: MR = 1.17 for DI water and MR = 1.21 for SC1 solution.

For both substrates, MR is greater than 1. Higher MR is calculated in SC1 than in DI water.

The magnitude of the forces and moments used here for a 63 nm PSL particle, bare silicon wafer, and SC1 is given below as an example.

The removal forces are drag force = 1.23×10^{-10} N, double-layer force: 1.16×10^{-10} N (repulsive), and the removal moment is 7.25×10^{-19} N.m

The adhesion force is 1.47×10^{-9} N and the adhesion moment is 5.28×10^{-19} N.m.

Using the removal efficiency vs MR plot by Lin,¹¹ the theoretical particle removal efficiencies are determined. The experimental and theoretical values for removal efficiency after 2 min using the megasonic tank are plotted in Fig. 5.

The removal model used here only accounts for Ekcort streaming, which is considered to be the dominant removal mechanism. There are two other streaming mechanisms: Schlichting streaming and microstreaming. Microstreaming, another important mechanism, is very difficult to predict and could contribute 10–30% to the removal. Thus, the removal moment used in this model is not the only removal force on the nanoparticle. So, the theoretical values for removal efficiency are slightly different from the experimental values but they follow the same trend. The theoretical and experimental results both show that particles on the Si-capping layer have lower MR than particles on bare silicon wafers in DI water. Also, on the same substrates, dilute SC1 gave a higher MR than DI water.

The double-layer force, which could be attractive or repulsive, also plays a role in the removal of particles. The measured particle and surface zeta potential is used in the calculation of the double-layer force. Also, the SC1 solution induces a larger repulsive interaction between surface and particle that results in larger MR compared to DI water.

The measured zeta potential values for pH 7 are as follows:

Bare silicon: –68 mV

4 nm Si-capping layer: –4 mV

The reason for the low surface potential (close to zero charge) for the 4 nm Si-capping layer is because of the conductive film underneath the Si cap. Figure 6 illustrates the experimental particle removal efficiency results as a function of time. After 2 min, an average removal efficiency of 99% using DI water and complete removal using SC1 is achieved for the case of bare silicon wafer. Due to a much lower repulsive double-layer force of the Si-cap surface,²⁷ the removal efficiency is lower compared to bare silicon.

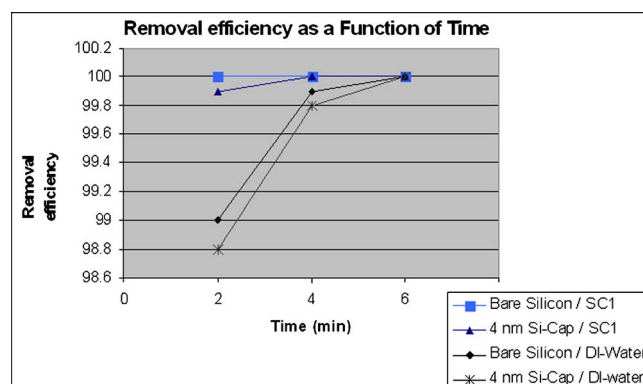


Figure 6. Particle removal efficiency of fluorescent PSL particles on bare silicon and 4 nm cap layer wafers as a function of time in DI water and SC1.

The other effective parameter in megasonic particle removal is the cleaning media. The use of SC1 instead of DI water provides higher removal efficiency for 63 nm PSL particles on both substrates due to the higher repulsive double-layer force in the case of using SC1. The results show that using SC1 reduces the cleaning time by 2 min.

The results show that the removal of nanoparticles takes a much longer time than sub- μm particles.^{28–30} Physical modeling has been used to understand this phenomenon. A computational fluid dynamic model is developed to investigate the time effect. Brownian motion is included in the particle-fluid interaction model. This model captures the particle behavior within the boundary layer. The particle detachment from the surface of the wafer is analyzed using the removal moment equations. Once the detachment is verified, the particle trajectory is analyzed using a particle transport model as a part of the CFD simulation. According to the simulation, removed particles undergo a circulatory and back and forth motion as shown in Fig. 7. The particle trajectory shows the redeposition of particles on the substrate. This redeposition results in a longer time to achieve complete removal.

The particle trajectory plot illustrated in Fig. 7 is a 2D model and it shows the redeposition of the particle after it travels $2 \mu\text{m}$ along the wafer. Point “A” is the original position of the particle. According to the simulation, the 63 nm particle deposits as much as six times on the surface of the wafer before it moves $2 \mu\text{m}$ toward the outer edge of the wafer. To assess the effect of particle size on the cleaning time, the trajectory of a larger particle (500 nm) is modeled under the same conditions. The particle trajectory shows that no redeposition occurs and that the particle is being carried away from the surface. This trajectory is shown in Fig. 8. Based on the results,

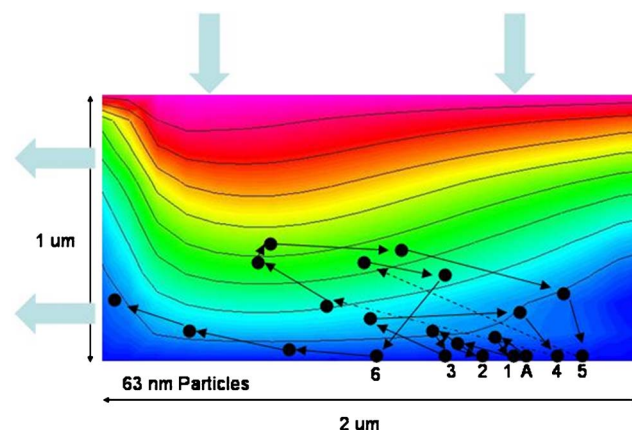


Figure 7. CFD simulation of the redeposition of 63 nm particles.

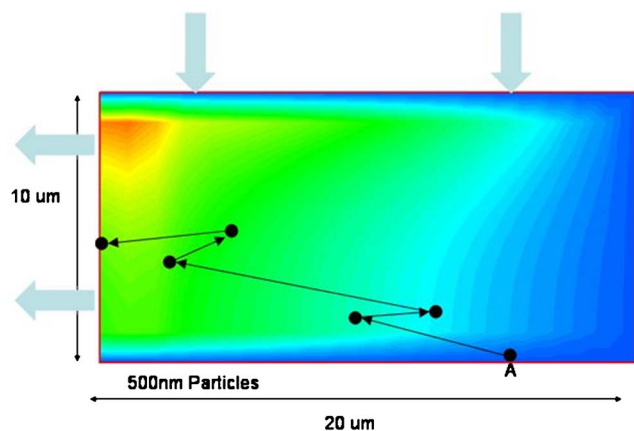


Figure 8. CFD simulation of the trajectory of 500 nm particles during cleaning.

the oscillatory path is minimal for the larger particle. The smoother trajectory has resulted in faster removal time for the 500 nm particle compared to the 63 nm nanoparticle.

Conclusions

The experimental results show higher than 99% removal of 63 nm PSL nanoparticles from bare silicon wafers and wafers with a 4 nm silicon cap layer. Particle removal from the 4 nm Si-cap substrate is slightly more difficult as compared to bare silicon wafer due to a lower double-layer repulsive force of the Si-cap surface. The MR analysis is in good agreement with the experimental results. The experiments also show that dilute SC1 results in higher MR than DI water due to the larger repulsive charge on the particle at a higher pH. The simulation shows that once a nanoparticle is detached from the substrate it undergoes oscillatory motion and multiple redepositions and removal takes place. The particle oscillatory motion and redeposition is the main reason for the long time required for nanoparticle removal as compared to μm and sub- μm -size particles. The modeling and experimental results show that 63 nm and larger PSL particles can be completely removed using acoustic streaming from bare silicon and 4 nm Si-cap layer wafers. According to the particle removal experiments, complete removal of the 63 nm PSL particles is achieved after 4 min in dilute SC1 and after 6 min in DI water for both substrates.

Acknowledgments

This work is supported by the National Science Foundation, Intel, and the NSF Center for Microcontamination Control industrial members, PCT Systems, Seagate, and Dupont EKC.

Northeastern University assisted in meeting the publication costs of this article.

References

1. The International Technology Roadmap for Semiconductors (ITRS), SIA (2004).
2. J. Olaf, *Acustica*, **7**, 253 (1957).
3. D. H. McQueen, *Ultrasonics*, **24**, 273 (1986).
4. I. Kashkoush, A. A. Busnaina, F. W. Kern, and R. F. Kunesch, *Ultrasonic Cleaning of Surfaces—An Overview, Particles on Surfaces*, Vol. 3, K. Mittal, Editor, pp. 217–237, Plenum, New York (1991).
5. G. W. Gale and A. A. Busnaina, *Part. Sci. Technol.*, **17**, 229 (1999).
6. A. A. Busnaina, I. I. Kashkoush, and G. W. Gale, *J. Electrochem. Soc.*, **142**, 2812 (1995).
7. A. A. Busnaina and G. W. Gale, *Part. Sci. Technol.*, **17**, 229 (1999).
8. A. A. Busnaina and G. W. Gale, *Part. Sci. Technol.*, **15**, 229 (1997).
9. M. Olim, *J. Electrochem. Soc.*, **144**, 3657 (1997).
10. J. M. Bernard, O. Guildkin, A. A. Busnaina, and J. Park, *Semiconductor Fabtech*, 23rd ed., pp. 77–79 (2004).
11. H. Lin, Ph.D. Thesis, Clarkson University, Potsdam, NY (2001).
12. W. L. Nyborg, *Acoustic Streaming*, Physical Acoustics, Vol II—Part B, W. P. Mason, Editor, Academic Press, New York (1965).
13. K. Bakhtari, O. Guldiken, P. Makaram, A. A. Busnaina, and J. Park, in *The Adhesion Society, Proceedings, 2005*, p. 404–406 (2005).
14. D. S. Rimai and D. J. Quesnel, *Fundamentals of Particle Adhesion*, Global Press (2001).
15. R. A. Bowling, *Particles and Surfaces Detection, Adhesion and Removal*, pp. 129–142, Plenum Press, New York (1988).
16. V. M. Muller, B. V. Derjaguin, and Y. P. Toporov, *Colloids Surf.*, **7**, 251 (1983).
17. K. L. Johnson, K. Kendall, and A. D. Roberts, *Proc. R. Soc. London, Ser. A*, **324**, 301 (1971).
18. S. Krishnan, A. A. Busnaina, D. S. Rimai, and D. P. DeMejo, *J. Adhes. Sci. Technol.*, **8**, 1357 (1994).
19. R. Hogg, T. W. Healy, and D. W. Fuerstenau, *Trans. Faraday Soc.*, **62**, 1638 (1966).
20. J. Gregory, *J. Chem. Soc., Faraday Trans. 2*, **69**, 1723 (1973).
21. J. Gregory, *J. Colloid Interface Sci.*, **51**, 44 (1975).
22. K. Bakhtari, R. Guldiken, A. A. Busnaina, and J. Park, *The Adhesion Society, Proceedings, 2005*, p. 115–117 (2005).
23. K. Bakhtari, O. Guldiken, A. A. Busnaina, and J. Park, *J. Electrochem. Soc.*, **153**, C603 (2006).
24. O. Guldiken, K. Bakhtari, A. A. Busnaina, and J. Park, *Solid State Phenom.*, **103–104**, 137 (2005).
25. M. Soltani and G. Ahmadi, *J. Adhes. Sci. Technol.*, **8**, 763 (1994).
26. F. Zhang, A. A. Busnaina, and G. Ahmadi, *J. Electrochem. Soc.*, **146**, 2665 (1999).
27. S. Lee, Y. Hong, J. Song, J. Park, A. A. Busnaina, G. Zhang, F. Eschbach, and A. Ramamoorthy, *Jpn. J. Appl. Phys., Part 1*, **44**, 5560 (2005).
28. A. A. Busnaina, in *Proceedings, SEMICON Korea, Seoul, Korea, Jan 21–23*, pp. 147–162 (2003).
29. J. M. Bernard, O. Guildkin, A. A. Busnaina, and J. Park, *Semiconductor Fabtech*, 23rd ed., pp. 77–79 (2004).
30. A. A. Busnaina, J. Park, A. Ramamoorthy, and G. Zhang, *Proceedings, 2nd International EUVL Symposium (CD)*, Antwerp, Belgium (2003).